

Heterogeneous Multi-Agent Reinforcement Learning with Attention for Cooperative and Scalable Feature Transformation

Tao Zhe
University of Kansas
Lawrence, KS, USA
taozhe@ku.edu

Huazhen Fang
Michigan State University
East Lansing, MI, USA
hfang@msu.edu

Kunpeng Liu
Clemson University
Clemson, SC, USA
kunpenl@clemson.edu

Qian Lou
University of Central Florida
Orlando, FL, USA
qian.Lou@ucf.edu

Tamzidul Hoque
University of Kansas
Lawrence, KS, USA
hoque@ku.edu

Dongjie Wang*
University of Kansas
Lawrence, KS, USA
wangdongjie@ku.edu

Abstract

Feature transformation enhances downstream task performance by generating informative features through mathematical feature crossing. Despite the advancements in deep learning, feature transformation remains essential, particularly for structured data, where deep models often struggle to capture complex feature interactions effectively. Prior literature on automated feature transformation has achieved notable success but often relies on heuristics or exhaustive searches, leading to inefficient and time-consuming processes. Recent works employ reinforcement learning (RL) to enhance traditional approaches through a more effective trial-and-error way. However, two key limitations remain: 1) Dynamic feature expansion during the transformation process, which introduces instability and increases the time complexity of the learning procedure for RL agents; 2) Insufficient cooperation and communication between agents, which results in suboptimal feature crossing operations and degraded model performance. To address them, we propose a novel heterogeneous multi-agent RL framework to enable cooperative and scalable feature transformation. The framework comprises three heterogeneous agents, grouped into two types, each designed to select essential features and operations for feature crossing. To enhance communication among these agents, we implement a shared critic mechanism that facilitates information exchange during the feature transformation process. This collaboration enables the agents to learn more intelligent and effective transformation policies. To handle the dynamically expanding feature space, we tailor multi-head attention-based feature agents to select suitable features for feature crossing. This design facilitates scalable decision-making and effective candidate selection based on comprehensive global feature space information. Additionally, we introduce a state encoding technique during the optimization process to stabilize and enhance the learning dynamics of the RL agents, resulting in more robust and reliable transformation policies.

*Corresponding author.

Permission to make digital or hard copies of all or part of this work for personal or classroom use is granted without fee provided that copies are not made or distributed for profit or commercial advantage and that copies bear this notice and the full citation on the first page. Copyrights for third-party components of this work must be honored. For all other uses, contact the owner/author(s).

KDD '26, Jeju, Korea

© 2026 Copyright held by the owner/author(s).

ACM ISBN 979-8-4007-1454-2/xx/xx

<https://doi.org/10.1145/...>

Finally, we conduct extensive experiments to validate the effectiveness, efficiency, robustness, and interpretability of our model. Our code and dataset are publicly available on GitHub¹.

CCS Concepts

• **Computing methodologies** → **Machine learning**.

Keywords

Feature Transformation, Multi-agent Reinforcement Learning, Automated Feature Engineering

ACM Reference Format:

Tao Zhe, Huazhen Fang, Kunpeng Liu, Qian Lou, Tamzidul Hoque, and Dongjie Wang. 2026. Heterogeneous Multi-Agent Reinforcement Learning with Attention for Cooperative and Scalable Feature Transformation. In *KDD '26*: ... ACM, New York, NY, USA, 11 pages. <https://doi.org/10.1145/...>

1 Introduction

Feature transformation creates more informative features by mathematically transforming the original ones. This enhances pattern distinguishability and improves model performance. Despite the remarkable success of deep learning, feature transformation remains essential for structured data (e.g., tabular data) [11] and scenarios requiring high interpretability or the integration of domain-specific knowledge. For instance, in finance, features like debt-to-income ratio and credit utilization are derived from raw data. These features enhance interpretability and improve the performance of tasks such as credit risk assessment and loan approval. In healthcare, risk scores are derived by transforming clinical measurements into interpretable features. These features support more accurate diagnosis and treatment planning. All of these examples demonstrate that feature transformation still plays an important role in real-world scenarios and AI applications.

Existing work on automated feature transformation can be categorized: 1) Expansion reduction methods [15, 20, 22], which expand the feature space by applying mathematical operations and then select the most suitable features to reduce the feature space size; 2) Iterative feedback loops [17, 18, 21, 33, 37], which iteratively refine features based on feedback from downstream tasks, optimized by RL or evolutionary algorithms; 3) AutoML-based methods [6, 12, 25, 38, 44, 50], which frame feature transformation as a

¹<https://github.com/Ricksanchez000/HAFT>

search problem for neural architectures and solve it using AutoML techniques. Among these, iterative-feedback paradigms excel at dynamically refining features over iterations. They can adapt to diverse downstream tasks and often yield effective feature spaces.

Recent studies have shown the effectiveness of RL in feature transformation [17, 19, 37, 42, 43, 46, 47]. Typically, RL agents are employed to select the necessary features and mathematical operations to generate new informative features. This process is repeated iteratively with the goal of optimizing downstream task performance, continuing until the maximum iteration limit is reached. However, existing RL-based methods still face two key challenges:

- **Challenge 1: Continuous dynamic expansion of the feature space during the iterative RL learning process.** During the feature transformation, the feature space undergoes continuous dynamic expansion over time. This expansion makes RL agents difficult and inefficient in identifying key features that are required for effective feature crossing.
- **Challenge 2: Insufficient cooperation and communication among different RL agents for policy learning.** Existing works often rely on purely local exchanges (e.g., selected features or operations from previous agents), limiting the agents’ awareness of the global feature space and resulting in suboptimal policies and feature spaces.

To address these challenges, we propose a **H**eterogeneous multi-**A**gent reinforcement learning framework for cooperative and scalable **F**eature **T**ransformation, referred to as **HAFT**. Specifically, we first design three RL agents, with two responsible for choosing candidate features and one for choosing mathematical operations. With feature choice facing an expanding space and operation choice using a static set, we develop two types of heterogeneous agents. This design ensures that each task is handled efficiently and effectively, enhancing the scalability and adaptability of the feature transformation process. Then, we propose an attention-based feature agent structure to adapt to the dynamically expanding feature space and identify the most suitable feature for the next feature crossing step. By focusing on relevant features and incorporating global context, this structure allows the agent to capture dynamic changes in the feature space and understand complex feature interactions for decision making. Moreover, we introduce a shared central critic for the RL agents to evaluate their decisions using unified information throughout the transformation process. By providing a global view of the feature space and incorporating the actions of other agents, the critic enhances communication and cooperation among them. This strategy enables each agent to make more informed and coordinated decisions, fostering effective feature transformation policies. To further stabilize and enhance the learning process, we propose a state encoding technique. This method mitigates significant state changes caused by feature space expansion, which stabilizes RL learning and improves the feature space exploration process.

To summarize, our contributions are threefold:

- **Problem:** We propose a new framework for automated feature transformation that leverages multi-agent cooperation to efficiently and scalably explore the feature space.
- **Algorithm:** We design a heterogeneous agent structure, customized based on the task of selecting features or operations. An attention-based feature agent structure is implemented to

adapt to the dynamically expanding feature space. Moreover, we propose a shared critic structure to enhance communication and cooperation among the agents.

- **Evaluation:** We conduct extensive experiments on 23 real-world datasets to validate the effectiveness of HAFT. The experimental results demonstrate the superiority of HAFT and highlight the indispensability of each of its components.

2 Problem Statement

We aim to develop an automated feature transformation framework that efficiently refines the feature space to maximize downstream task performance. Given a dataset $\mathcal{D}\langle\mathcal{F}, y\rangle$, where \mathcal{F} represents input features and y is the target variable, and a mathematical operation set \mathcal{O} (e.g., addition, multiplication, division), the objective is to generate an optimal feature set \mathcal{F}^* that maximizes ML task A ’s performance metric P^A . The optimization goal can be formulated as follows:

$$\mathcal{F}^* = \arg \max_{\hat{\mathcal{F}}} \left(P^A(\hat{\mathcal{F}}, y) \right), \quad (1)$$

where $\hat{\mathcal{F}}$ is a feature subset derived from the union of the transformed new features \mathcal{F}^g and the original feature set \mathcal{F} . \mathcal{F}^g is generated by applying the mathematical operations from \mathcal{O} to features from the original feature set \mathcal{F} for feature crossing. For example, multiplying *length* and *width* creates a new feature *area=length×width*. After reaching the maximum iteration limit, the feature space with the highest downstream task performance is output as \mathcal{F}^* .

3 Methodology

3.1 Framework Overview

Figure 1 demonstrates the architecture of HAFT. In the iterative optimization process, three heterogeneous cascading agents collaborate to learn the feature transformation policy. Two feature agents identify candidate features, while the operation agent selects a mathematical operation. Given the continuous evolution of the feature space, HAFT incorporates a multi-head attention-based feature agent structure to select features that contribute effectively to feature transformation using global information. This design maintains a consistent agent structure, ensuring effectiveness and scalability without structural modifications. To manage the complex dependencies among agents, a shared central critic integrates global feature space information and agent decisions to guide and enhance policy learning. The selected operation is then applied to the candidate features to generate new and informative features in each iteration. The optimization process will be guided by the performance of downstream tasks. The entire process is repeated until either the optimal feature space is identified or the maximum iteration limit is reached. Finally, the feature space with the highest downstream task performance is output as the optimal solution.

3.2 Heterogeneous Cascading Agents for Candidate Features and Operations

To handle dynamic and complex nature of automated feature transformation, we design a cascading structure with three heterogeneous agents: a head feature agent, an operation agent, and a tail feature agent. They collaborate iteratively to identify candidate

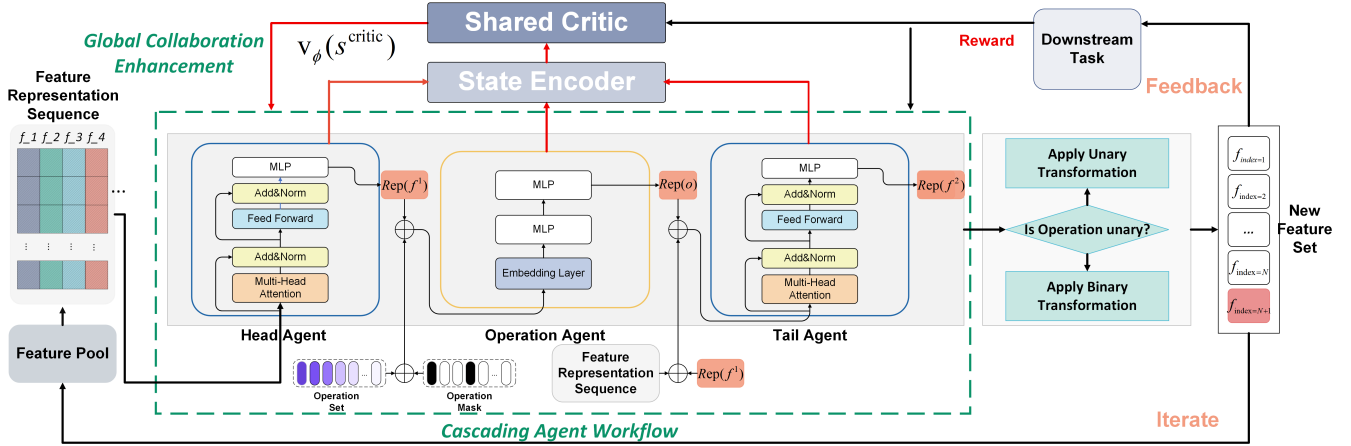


Figure 1: Framework Overview. HAFT consists of three heterogeneous agents: two feature agents that select candidate features and one operation agent that determines a mathematical operation. A central critic leverages global information from the current feature space to coordinate the agents and enhance policy learning. This feature transformation process continues iteratively until an optimal feature set is identified or the iteration limit is reached.

features and operations for feature transformation. Each agent is specialized for a specific role to better capture global context, grasp dependencies, and adapt to the dynamic evolving feature spaces.

Cascading Agent Workflow: At the t -th iteration, the three agents collaborate to choose candidate features and operation for feature crossing. In the following, we first outline the workflow and define the state, action, and reward for each agent in the process. **Head feature agent** selects a feature f_{t-1}^1 from the feature set \mathcal{F}_{t-1} based on the information of global feature space. Within this agent, **state:** $s_t^1 = \text{Rep}(\mathcal{F}_{t-1})$, where $\text{Rep}(\mathcal{F}_{t-1})$ is the representation of the current feature space. Here, $\text{Rep}(\mathcal{F}_{t-1})$ is obtained by statistical descriptors of the feature set (e.g., mean and variance). **action:** $a_t^1 = f_{t-1}^1$ is the selected feature from the feature set \mathcal{F}_{t-1} . **Operation agent** selects an operation o_t from the operation set \mathcal{O} based on the decision of the head feature agent and the current dynamic mask (in equation 3). Within this agent, **state:** $s_t^o = c_t \oplus \text{Rep}(f_{t-1}^1)$, which is the concatenation of the representation of the current dynamic mask and the first candidate feature. **action:** $a_t^o = o_t$ is the selected feature from the mathematical operation set \mathcal{O} . **Tail feature agent** selects second feature f_{t-1}^2 from the feature set \mathcal{F}_{t-1} based on the decisions of the head feature agent, operation agent, and the current feature space representation. Within this agent, **state:** $s_t^2 = \text{Rep}(\mathcal{F}_{t-1}) \oplus \text{Rep}(f_{t-1}^1) \oplus \text{Rep}(o_t)$, where $\text{Rep}(o_t)$ is the one-hot encoding vector for the selected operation. **action:** $a_t^2 = f_{t-1}^2$ is the selected feature from the feature set \mathcal{F}_{t-1} . **Reward:** The three agents are all driven by the downstream machine learning task performance V_A . They equally share the reward, defined as $\mathcal{R}(s_t^1, a_t^1) = \mathcal{R}(s_t^o, a_t^o) = \mathcal{R}(s_t^2, a_t^2) = P_t^A$.

3.2.1 Multi-Head Attention-Based Feature Agent. Why dynamic evolving feature space matters? During the iterative process, the size of the feature space changes after each iteration. This dynamic nature makes it challenging to design an agent structure that can handle variable input sizes and capture complex feature interactions effectively. Prior research [37] employs group-wise clustering to address the dynamic changes within the feature space.

While effective in capturing high-level group structures, this approach struggles with scalability and modeling fine-grained feature relationships. Thus, we propose a multi-head attention-based [36] agent structure to address these limitations. In the following, we show the calculation process using the feature space at iteration t . To simplify notation, we omit t , using \mathcal{F} to represent \mathcal{F}_t .

Let $\mathbf{H}_0 = \text{Rep}(\mathcal{F}) \in \mathbb{R}^{N \times d}$ be the initial feature matrix, where N is the number of features and d is the representation dimension. A Transformer Encoder Layer applies multi-head self-attention to the feature matrix to capture the complex interaction between features. Concretely, use \mathbf{H}_k to denote the hidden representations after the k^{th} encoder block. Each block has h attention heads. For head $j \in \{1, 2, \dots, h\}$, we compute: $\mathbf{Q}_k^j = \mathbf{H}_{k-1} \mathbf{W}_{k,Q}^j$, $\mathbf{K}_k^j = \mathbf{H}_{k-1} \mathbf{W}_{k,K}^j$, and $\mathbf{V}_k^j = \mathbf{H}_{k-1} \mathbf{W}_{k,V}^j$, where $\mathbf{W}_{k,Q}^j, \mathbf{W}_{k,K}^j, \mathbf{W}_{k,V}^j \in \mathbb{R}^{d \times (d/h)}$ are learnable projection matrices for queries, keys, and values. Each head operates independently on these projections, enabling the model to capture various aspects of the relationships among features. The scaled dot-product attention for head j is given by: $\mathbf{H}_k^j = \text{softmax}\left(\frac{\mathbf{Q}_k^j (\mathbf{K}_k^j)^\top}{\sqrt{d/h}}\right) \mathbf{V}_k^j$. We then concatenate the outputs and pass them to a feed-forward function:

$$\mathbf{H}_k = \text{FFN}\left(\text{Concat}(\mathbf{H}_k^1, \dots, \mathbf{H}_k^h)\right). \quad (2)$$

This yields the representation for the next layer. Stacking K such blocks results in the final encoder output \mathbf{H}_K . We input \mathbf{H}_K into a linear layer with softmax activation function to learn a distribution over all features. The feature agent samples the optimal feature for crossing based on the learned distribution. This design adapts to dynamic changes in the feature space, as self-attention assigns weights based on feature relevance without requiring a fixed input size or manual indexing, ensuring scalability for large feature space.

3.2.2 MLP-Based Operation Agent. Unlike feature agents, the operation agent selects an operation from a fixed set, making its task

simpler than choosing features. To accommodate this difference, we design an MLP-based operation agent. This heterogeneity in agent structure allows task-specific customization, which enhances policy learning and improves both feature and operation selection efficiency. Since the input size is fixed, we design an MLP-based operation policy network with a *dynamic mask* to enable both informed and valid operation selection. Certain operations may be invalid for specific features (e.g., `sqrt` is invalid if the feature contains negative values). To handle this, we define a dynamic action mask $\mathbf{c} \in \{0, 1\}^m$, where m is the number of predefined operations:

$$\mathbf{c} = (c_1, c_2, \dots, c_m), \quad c_i = \begin{cases} 1, & \text{if the } i\text{-th operation is valid,} \\ 0, & \text{otherwise.} \end{cases} \quad (3)$$

The input of the policy network is the concatenation of the selected head feature representation and the mask \mathbf{c} . This combined input is processed by a feed-forward neural network that outputs logits for each operation. For any invalid operation (i.e., $c_i = 0$), a large negative constant is added to its logit, effectively reducing its selection probability to near zero. This mechanism prevents invalid operations and overly deterministic policies, ensuring valid transformations and a more stable policy-learning process.

3.3 Enhancing Collaboration with a Shared Critic and Advantage Decomposition

Why a shared central critic matters? Existing works [37] on automated feature transformation rely on partial information (e.g., decisions from previous agents) to coordinate and learn transformation policies. However, convergence in this setting is particularly challenging, as each agent’s policy is influenced not only by preceding agents but also by subsequent ones, creating complex interdependencies. To improve communication among agents and learn better feature transformation policies, a shared central critic module is essential. This necessitates robust credit assignment and alignment mechanisms. Unlike conventional multi-agent systems or feature-selection RL—where action spaces remain fixed and counterfactual baselines are straightforward to define—feature transformation presents unique difficulties. The dynamic expansion of the feature pool throughout the learning process makes credit assignment substantially more complex, as each agent’s contribution becomes increasingly entangled with the evolving feature space. This contrasts with typical multi-agent settings where individual contributions to shared rewards are more readily identifiable or where counterfactual reasoning can be more directly applied.

To address these unique challenges, we apply a **Shared Critic with multi-agent advantage decomposition and a sequential policy-update scheme**[23, 48]. The critic consumes aggregated global information and outputs a single scalar value estimate:

$$\hat{V}_t = V_\phi(s^{\text{critic}}), \quad (4)$$

which serves as a unified baseline for advantage estimation. Each agent (head feature agent, tail feature agent, and operation agent) still acts on its local observation, but the centralized perspective of the Shared Critic aligns their learning toward producing high-quality transformations. With advantage decomposition, subtracting \hat{V}_t from individual returns yields clearer reward attribution,

stabilizes training, reduces non-stationarity, and strengthens collaboration. Building on this design, we now detail each agent’s update procedure within our framework.

Agents Update. We adopt the customized HAPPO algorithm to update our three agents, as it effectively addresses the complexity and instability inherent in our dynamic multi-agent environment while maintaining theoretical monotonic improvement guarantees. Its clipped objective function confines policy updates within a trust region, preventing destabilizing shifts during training. We employ the Generalized Advantage Estimation (GAE) advantage function to compute the joint advantage function \hat{A} , which balances bias and variance through its exponential weighting scheme. To utilize the advantage decomposition in our setting, we sequentially update our agents. While the order can be randomized in theory, we fix a consistent order (head feature agent \rightarrow operation agent \rightarrow tail feature agent) for simplicity. For the first agent in the sequence (e.g., the feature agent), we define: $M_t^1 = \hat{A}_t$, and the importance-sampling ratio: $\rho_t^1(\theta^1) = \frac{\pi_{\theta^1}(a_t^1|s_t^1)}{\pi_{\theta_{\text{old}}^1}(a_t^1|s_t^1)}$. The head feature agent’s clipped objective is then:

$$L_1(\theta^1) = \mathbb{E}_t \left[\min(\rho_t^1(\theta^1) M_t^1, \text{clip}(\rho_t^1(\theta^1), 1-\epsilon, 1+\epsilon) M_t^1) \right]. \quad (5)$$

After updating the feature agent’s parameters $\theta_{\text{old}}^1 \rightarrow \theta_{\text{new}}^1$, we adjust the advantage for the next agent (e.g., the operation agent)

to account for the updated policy: $M_t^{\text{op}} = \frac{\pi_{\theta_{\text{new}}^1}(a_t^1|s_t^1)}{\pi_{\theta_{\text{old}}^1}(a_t^1|s_t^1)} \cdot \hat{A}_t$. The operation agent’s ratio and objective are defined analogously, following the same clipped formulation. $\rho_t^o(\theta^o) = \frac{\pi_{\theta^o}(a_t^o|s_t^o)}{\pi_{\theta_{\text{old}}^o}(a_t^o|s_t^o)}$,

$$L_o(\theta^o) = \mathbb{E}_t \left[\min(\rho_t^o(\theta^o) M_t^o, \text{clip}(\rho_t^o(\theta^o), 1-\epsilon, 1+\epsilon) M_t^o) \right] \quad (6)$$

After updating the operation agent’s parameters $\theta_{\text{old}}^o \rightarrow \theta_{\text{new}}^o$, we form the tail feature agent’s decomposed advantage: $M_t^2 = \frac{\pi_{\theta_{\text{new}}^o}(a_t^o|s_t^o)}{\pi_{\theta_{\text{old}}^o}(a_t^o|s_t^o)} \cdot \frac{\pi_{\theta_{\text{new}}^1}(a_t^1|s_t^1)}{\pi_{\theta_{\text{old}}^1}(a_t^1|s_t^1)} \cdot \hat{A}_t$. Define its ratio: $\rho_t^2(\theta^2) = \frac{\pi_{\theta^2}(a_t^2|s_t^2)}{\pi_{\theta_{\text{old}}^2}(a_t^2|s_t^2)}$.

The tail feature agent’s clipped objective becomes:

$$L_2(\theta^2) = \mathbb{E}_t \left[\min(\rho_t^2(\theta^2) M_t^2, \text{clip}(\rho_t^2(\theta^2), 1-\epsilon, 1+\epsilon) M_t^2) \right]. \quad (7)$$

This sequential scheme ensures that each agent’s update accounts for the changes introduced by previously updated agents, mitigating the challenge of conflicting policy update of each agent. To refine the reward for our feature transformation task, we incorporate characteristics of the generated feature space. Specifically, an ideal feature space generally has low information redundancy and high relevance to the predictive labels. We quantify both using mutual information MI : The **Information redundancy** is defined as the average pairwise MI among features: $Id = \frac{1}{|N|^2} \sum_{f_i, f_j \in N} MI(f_i; f_j)$, where N is the feature subset, f_i is the i -th feature. The **information relevance** is the average MI between features and labels: $Iv = \frac{1}{|N|} \sum_{f_i \in N} MI(f_i; y)$, where y is the label vector. To encourage exploration, we also add an entropy term $H(\pi_{\theta^{(i)}})$. Our final loss function for optimizing the three agents is

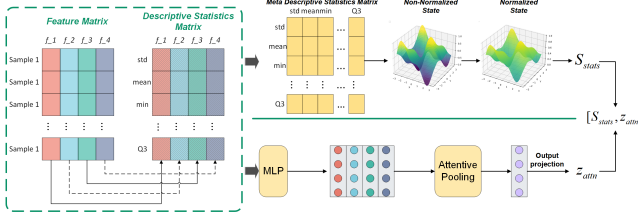


Figure 2: Two-branch state encoder. A statistics branch expands the dynamic feature set and normalizes it to $\mathbb{R}^{1 \times 49}$; an attention branch embeds features, applies multi-head attention, and pooling to obtain z_{attn} . Finally create input $s^{critic} = [S_{stats}, z_{attn}]$.

thus defined as follows: For each agent $i \in \{\text{feat_h}, \text{op}, \text{feat_t}\}$, the policy loss is given by:

$$\mathcal{L}_{\text{policy}}^{(i)}(\theta^{(i)}) = -L_{\text{CLIP}}^{(i)} - \beta_i \mathbb{E}_t [H(\pi_{\theta^{(i)}})] + \beta_{\text{Id}} Id - \beta_{\text{IV}} Iv, \quad (8)$$

where $L_{\text{CLIP}}^{(i)}$ is one of the clipped surrogates defined above, β_i controls entropy regularization. And finally the agent’s policy network parameters are updated via gradient descent optimization.

Shared Critic Update. The shared critic is updated by minimizing the mean-squared error (MSE) between the predicted value and the computed returns from trajectories:

$$\mathcal{L}_{\text{value}}(\phi) = \frac{1}{2} \mathbb{E}_t \left[\left(V_{\phi}(s_t^{critic}) - \hat{R}_t \right)^2 \right], \quad (9)$$

where \hat{R}_t represents the returns computed using GAE. Specifically, $\hat{R}_t = \hat{A}_t + V_{\phi}(s_t^{critic})$, where \hat{A}_t is the GAE advantage estimate computed from the collected trajectory rewards and bootstrapped values. The network parameters ϕ are updated via gradient descent.

3.4 State Encoding for Shared Critic

As outlined in the shared critic section, the aggregated global information of our multi-agent feature transformation system represents the current feature set environment after each iteration, reflecting the updated features generated by the agents. Specifically, as the number of features increases by one after each step, the resulting shift in the input state distribution can destabilize the critic’s evaluation process. This instability may manifest as erratic output values and, in extreme cases, exploding gradients, which can corrupt the overall training of the framework. In addition to these aggregates, heuristic signals are also essential for reliable evaluation. To provide the critic with a stable yet expressive view of the evolving space, we construct a two-branch, permutation-robust state as shown in Fig. 2: i) a distributional-statistics branch that converts the variable-length pool into a fixed, normalized summary $S_{stats} \in \mathbb{R}^{1 \times 49}$, ii) an attention-based interaction branch that embeds per-feature tokens with multi-head attention and permutation-invariant pooling to produce $z_{attn} \in \mathbb{R}^{1 \times 49}$. The final critic input is the concatenation :

$$s^{critic} = [S_{stats}, z_{attn}] \quad (10)$$

Distributional Statistics & Normalization. To construct S_{stats} , we propose a two-stage approach. First, we expand the dynamic feature set by computing a series of descriptive statistics, including the mean, standard deviation, minimum, maximum, and the first,

second and third quartiles. Following the first step, we calculate the descriptive statistics again row by row. This statistical summary effectively condenses the raw, variable-length feature set into a fixed set of informative metrics. Second, we apply a normalization step (e.g., min-max normalization or z-score normalization) to these statistics. This normalization is crucial as it scales each statistic to a similar range, preventing any single metric from disproportionately affecting the critic’s output and helping to control gradient magnitudes. The combined process produces a fixed input state representation with a shape of $\mathbb{R}^{1 \times 49}$.

Attention-based Interaction. While aggregated global statistics summarize each feature, they do not capture feature–feature interactions, which are critical for constructing a refined feature space. Therefore, we construct z_{attn} by adopting an attention-based encoder: each feature is first mapped to a continuous token embedding; the set of embeddings is then processed with multi-head attention to produce context-aware representations. A permutation-invariant pooling operation (e.g., attention pooling or mean–max pooling) aggregates them into a fixed-length vector, which is concatenated with the statistics-based summary to form the shared critic’s state.

The resulting state representation stabilizes training by fixing the input dimensionality regardless of dynamic feature size, and normalizing scales so no statistic dominates the gradients. In practice, it provides a compact, informative signal that improves value estimation and credit assignment, simplifies the critic architecture, and leads to more reliable convergence for our system.

4 Experiments

4.1 Experiment Setup

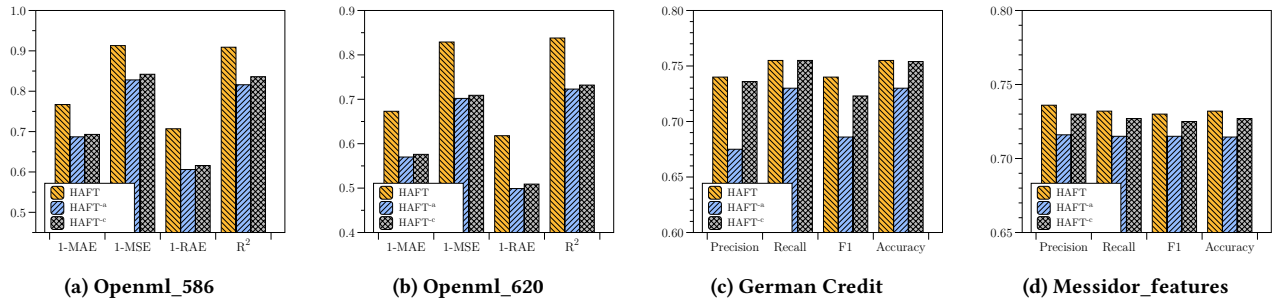
4.1.1 Datasets. We use 23 publicly available datasets from UCI [34], LibSVM[24], Kaggle[16], and OpenML[29] to conduct our experiments. The 23 datasets involve 14 classification tasks and 9 regression tasks. Table 1 reflects the statistics of the data.

4.1.2 Evaluation Metrics. We adopt standard evaluation metrics to ensure a comprehensive analysis of our model’s performance. Regression tasks were evaluated using the following metrics: 1-Relative Absolute Error (1-RAE) [37], 1-Mean Absolute Error (1-MAE), 1-Mean Squared Error (1-MSE) and coefficient of determination (R^2). For classification tasks, assessment was conducted using Precision, Recall, F1-score and Accuracy. The formulae for the F1-score and 1-RAE are given by: $F_1 = 2 \cdot \frac{\text{Precision} \cdot \text{Recall}}{\text{Precision} + \text{Recall}}$ and $1\text{-RAE} = 1 - \frac{\sum_{i=1}^n |y_i - \tilde{y}_i|}{\sum_{i=1}^n |y_i - \bar{y}_i|}$, where y_i , \tilde{y}_i , and \bar{y}_i represent the ground truth, predictions, and the mean of the ground truth respectively.

4.1.3 Baseline Model. We compare our method with 8 widely-used feature transformation methods. 1) **RDG** generates feature-operation-feature transformation records randomly to create a new feature space. 2) **ERG** applies operations to each feature to expand the feature space and selects the crucial features as the new feature set. 3) **LDA** [3] is a matrix factorization-based method that obtains the factorized hidden state as the generated feature space. 4) **AFAT** [15] is an enhanced version of ERG that repeatedly generates new features and uses multi-step feature selection to identify informative ones. 5) **NFS** [6] models the transformation sequence of each feature and uses reinforcement learning (RL) to optimize the entire

Table 1: Overall Performance. ‘C’ for classification and ‘R’ for regression.

Dataset	Source	C/R	Samples	Features	RDG	ERG	LDA	AFAT	NFS	TTG	GRFG	DIFER	HAFT
Higgs Boson	UCIrvine	C	50000	28	0.695	0.702	0.513	0.697	0.691	0.699	<u>0.707</u>	0.669	0.709
Amazon Employee	Kaggle	C	32769	9	0.932	0.932	0.916	0.930	0.932	<u>0.933</u>	0.932	0.929	0.943
PimaIndian	UCIrvine	C	768	8	0.751	0.735	0.729	0.732	<u>0.791</u>	0.745	0.754	0.760	0.794
SpectF	UCIrvine	C	267	44	0.760	0.788	0.665	0.760	<u>0.792</u>	0.760	0.776	0.766	0.876
SVMGuide3	LibSVM	C	1243	21	0.806	<u>0.818</u>	0.635	0.794	0.786	0.798	0.812	0.773	0.837
German Credit	UCIrvine	C	1001	24	<u>0.701</u>	0.662	0.596	0.639	0.649	0.644	0.667	0.656	0.740
Credit Default	UCIrvine	C	30000	25	0.802	0.803	0.743	0.804	0.801	0.798	<u>0.806</u>	0.796	0.807
Messidor_features	UCIrvine	C	1150	19	0.627	<u>0.692</u>	0.463	0.657	0.650	0.655	0.680	0.660	0.730
Wine Quality Red	UCIrvine	C	999	12	<u>0.496</u>	0.485	0.401	0.480	0.451	0.467	0.454	0.476	0.561
Wine Quality White	UCIrvine	C	4900	12	0.524	<u>0.527</u>	0.438	0.516	0.525	0.521	0.518	0.507	0.543
SpamBase	UCIrvine	C	4601	57	0.906	0.917	0.889	0.912	<u>0.925</u>	0.919	0.922	0.912	0.928
AP-omentum-ovary	OpenML	C	275	10936	0.820	<u>0.849</u>	0.716	0.813	0.830	0.830	0.830	0.833	0.879
Lymphography	UCIrvine	C	148	18	0.108	<u>0.202</u>	0.144	0.149	0.166	0.148	0.136	0.150	0.397
Ionosphere	UCIrvine	C	351	34	0.942	<u>0.957</u>	0.743	0.942	0.943	0.932	0.956	0.905	0.957
Housing Boston	UCIrvine	R	506	13	<u>0.434</u>	0.410	0.020	0.401	0.428	0.396	0.409	0.381	0.476
Airfoil	UCIrvine	R	1503	5	0.519	0.519	0.207	0.507	0.520	0.500	0.521	<u>0.528</u>	0.548
Openml_618	OpenML	R	1000	50	0.472	<u>0.561</u>	0.052	0.473	0.467	0.467	0.577	0.408	0.475
Openml_589	OpenML	R	1000	25	0.509	0.610	0.011	0.508	0.503	0.504	0.627	0.463	<u>0.555</u>
Openml_616	OpenML	R	500	50	0.070	0.193	0.024	0.162	0.147	0.156	0.372	0.076	<u>0.271</u>
Openml_607	OpenML	R	1000	50	0.521	0.549	0.107	0.509	0.518	0.522	<u>0.555</u>	0.476	0.618
Openml_620	OpenML	R	1000	25	0.511	0.546	0.029	0.527	0.513	0.512	0.619	0.442	<u>0.618</u>
Openml_637	OpenML	R	500	50	0.136	0.064	0.043	0.161	0.146	0.144	0.307	0.072	<u>0.300</u>
Openml_586	OpenML	R	1000	25	0.568	0.624	0.110	0.553	0.542	0.544	<u>0.646</u>	0.482	0.707

**Figure 3: Influence of Shared Critic and Advantage Decomposition**

feature generation process. 6) **TTG** [21] formulates the transformation process as a graph and implements an RL-based search method to identify the best feature set. 7) **GRFG** [37] utilizes three collaborative reinforcement agents for feature generation and introduces a feature grouping strategy to accelerate agent learning. 8) **DIFER** [50] embeds randomly generated feature transformation records using a seq2seq model and employs gradient search to identify the best feature set. Besides that, to validate the necessity of each component of HAFT, we develop three model variants: a. **HAFT^{-c}** replaces the shared critic in HAFT with separate critics for each agent; b. **HAFT^{-a}** removes the advantage decomposition component from HAFT while retaining the shared critic. c. **HAFT^{-u}** only utilize the S_{stats} as the shared critic input.

4.1.4 Experimental Settings. All experiments are conducted on an Ubuntu 22.04.5 LTS operating system, powered by an AMD Ryzen Threadripper PRO 7965WX 24-core processor, using Python 3.12.7 and PyTorch 2.5.1 as the framework.

4.1.5 Hyperparameters and Reproducibility. The operation set includes square root, square, cosine, sine, tangent, exponential, cube, logarithm, reciprocal, quantile transformation, min–max scaling, sigmoid, addition, subtraction, multiplication, and division. We cap the process at 100 episodes, each with up to 25 steps, and select the top 20 features using a mutual-information-based metric to evaluate downstream performance. The entropy coefficient ranges from 0.01 to 0.3, and we explore learning rates of $1e-3$, $1e-4$, and $1e-5$ for both the feature agent and operation agent, the dimension for $z_{attn} \leq 49$ depending on the dataset. In terms of network architecture, the feature agent employs two Transformer encoder layers and one MLP projection layer. Meanwhile, the shared critic consists of four MLP layers, while the operation agent comprises two MLP layers, each employing LeakyReLU as the activation function. The parameters of all baseline models are configured according to the default settings specified in the corresponding papers, ensuring consistency in evaluation settings [45].

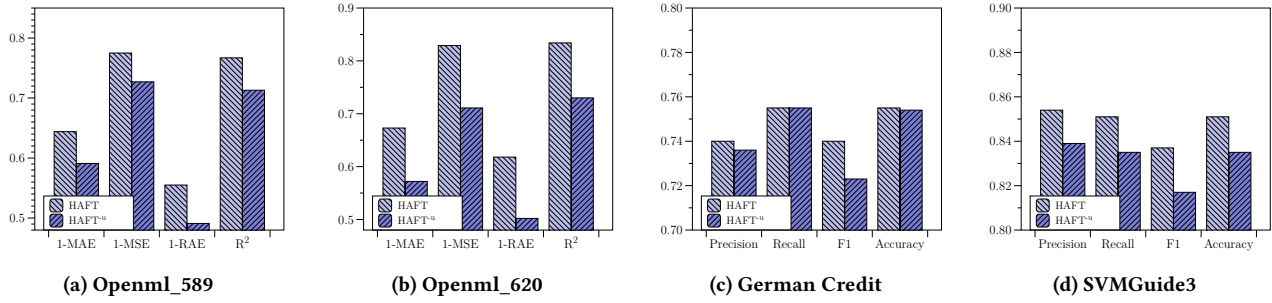


Figure 4: Influence of Different State Encoding

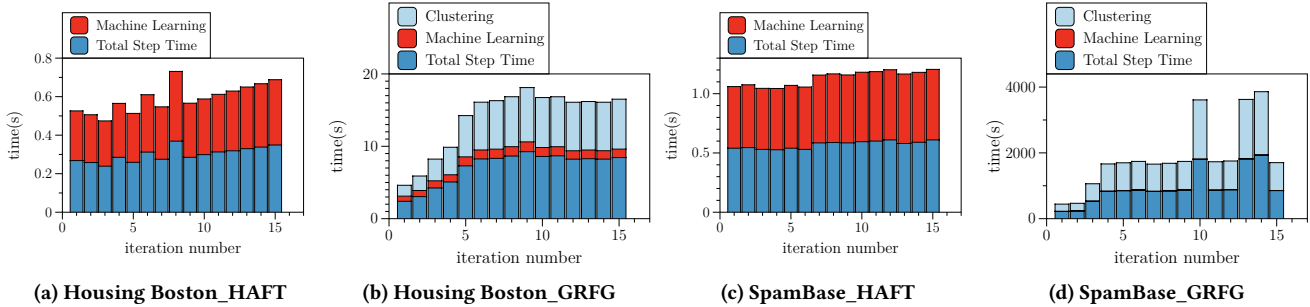


Figure 5: Time Complexity Comparison between HFT and GRFG

4.2 Experiment Results

4.2.1 Overall Performance. This experiment aims to answer the following question: *Can HFT construct a better feature space to improve downstream task performance?* Table 1 shows the experimental results in terms of F1 score or 1-RAE. (The bold/underline denotes best/second performance). We observe that HFT consistently outperforms other baselines across most domains and tasks while maintaining a stable top ranking. There are two potential reasons for the experimental observation: 1) the multi-head attention-based feature agent structure enables feature agents to focus on more significant features, leading to the generation of new informative features. 2) the shared critic mechanism improves communication and coordination among agents, facilitating the learning of a more effective feature transformation policy. Another notable observation is that, unlike HFT, the other models fail to maintain a stable performance rank throughout our experiments. This observation reflects the effectiveness of HFT in learning superior transformation strategies compared to other methods. In summary, this experiment demonstrates that HFT effectively refines the feature space to further enhance downstream tasks.

4.2.2 Ablation Study 1: Shared Critic. This experiment aims to answer: *Does a shared critic and advantage decomposition update improve agent communication and lead to more effective feature transformation policies over separate critics?* To answer this question, we develop model variant HFT^{-c}, which replaces the shared critic with separate critics for each agent, and HFT^{-a} which removes the advantage decomposition component from HFT while retaining the shared critic. We report the comparison results in terms of F1 score or 1-RAE on two regression datasets (e.g., Openml_586, Openml_620) and two classification datasets (e.g., German Credit, Messidor_features). Figure 3 presents the experimental results in

terms of corresponding evaluation metrics. We find that HFT consistently beats HFT^{-c} and HFT^{-a} across various datasets, and HFT^{-a} and HFT^{-c} perform on par with each other. This observation can be explained by two key mechanisms: The shared critic provides global guidance, and there might also exist updating direction conflict, while the advantage decomposition scheme enhances cooperation through more informative reward signals. This leads to the development of reliable feature-transformation policies, resulting in superior feature spaces. In summary, this experiment shows that the shared critic is essential for performance.

4.2.3 Ablation Study 2: Shared Critic States. This experiment aims to answer: *Does incorporating interaction information into the shared critic state improve feature transformation performance?* To address this question, we create the model variant HFT^{-u} by removing the interaction component of our shared critic’s state input. We then compare the performance of HFT and HFT^{-u} across two regression tasks (i.e., Openml_589 and Openml_620) and two classification tasks (i.e., German Credit and SVMGuide3). Figure 4 shows the comparison results in terms of F1 score or 1-RAE. We observe that HFT surpasses HFT^{-u} in most cases across all metrics. A plausible reason is that appending interaction information, alongside statistical representations of the feature space, helps to enrich the input to the shared critic, enabling it to better assess the quality of transformed features and guide the agent system more effectively. In summary, this experiment shows that incorporating interaction information is a beneficial design choice in HFT.

4.2.4 Robustness Check. This experiment aims to answer: *Does HFT exhibit robustness when confronted with various machine learning models serving as downstream tasks?* To answer this question, we replace the downstream ML model with Random Forest (RF) [4], XGBoost (XGB) [5], Support Vector Machine (SVM) [7], K-Nearest

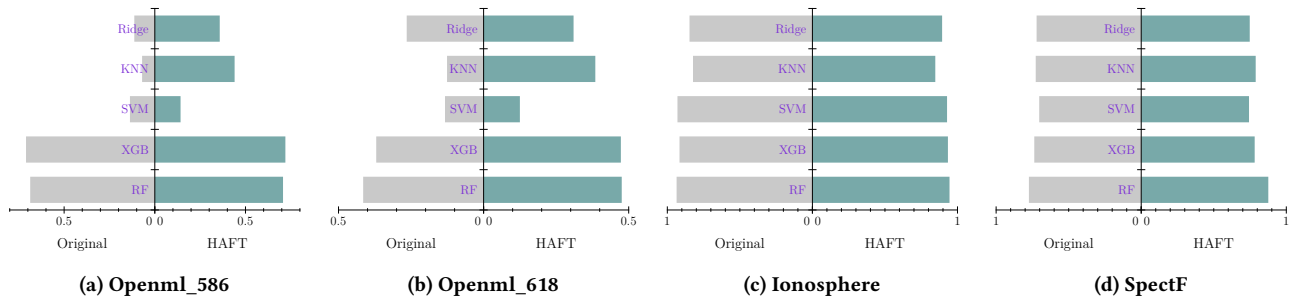
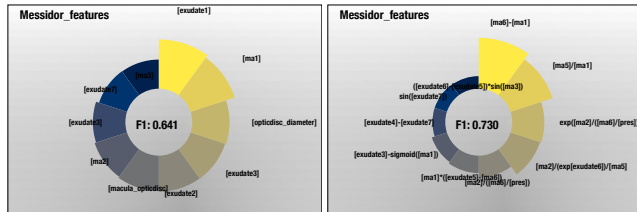


Figure 6: Robustness Check of HAFT when confronted with different downstream ML models in terms of F1 score and 1-RAE



(a) Original Feature Space (b) Reconstructed Feature Space
Figure 7: Case Study of Messidor_features dataset

Neighbors (KNN) [8], and Ridge Regression (Ridge) [14], respectively. Figure 6 presents the comparison results in terms of F1 score or 1-RAE on Openml_586, Openml_618, Ionosphere, and SpectF datasets. We find that regardless of changes in downstream models, HAFT consistently refines the feature space and achieves better results than the original feature space. The underlying reason is that HAFT can customize feature transformation policies to the specific characteristics of downstream models, resulting in more effective feature spaces. Thus, this experiment demonstrates the robustness of HAFT across different downstream models.

4.2.5 Scalability Analysis. This experiment aims to address the question: *Does HAFT exhibit better scalability than GRFG in refining the feature space?* GRFG is the algorithm most similar to HAFT, utilizing a group-wise feature generation strategy to refine the feature space. To further analyze scalability, we conduct experiments to compare the time costs of key components in GRFG and HAFT over 15 iterations on the Housing Boston and SpamBase datasets. Figure 5 presents the results of the time complexity comparison. We observe that the time cost per iteration of HAFT is significantly lower than that of GRFG, with GRFG requiring significantly more time. The primary reason for this observation is that clustering is the most time-consuming step in GRFG, as shown in Figure 5. Even with the high time cost in GRFG, its performance is still worse than HAFT. This observation suggests that although GRFG’s clustering strategy aims to refine the feature space group-wise, many of the generated features are ineffective for refinement. In contrast, HAFT utilizes multi-head attention to capture complicated feature interactions to select suitable features for feature crossing. Thus, HAFT is much more scalable and applicable in realistic scenarios.

4.2.6 Case Study. This experiment aims to answer: *Can HAFT generate an explainable and traceable feature space?* We select the top 10 essential features using mutual information as rank criteria for prediction in both the original and HAFT transformed feature spaces

of the Messidor_features dataset for comparison. Figure 7 shows the comparison results, where larger pie slices indicate higher feature importance. We find that all of the critical features in the new feature space were generated by HAFT resulting in a 13.9% improvement in downstream machine learning performance. This indicates that HAFT transforms features to refine the feature space. We also observe that one of the key features in the newly generated feature space is derived from the original feature [‘ma1’]. This indicates that HAFT is capable of tracing and explaining the transformed feature by checking its name. In our case, [‘ma1’] indicates MA detection at a 0.5 confidence level, and [‘[ma6]–[ma1]’] and [‘[ma5]/[ma1]’] reveals a traceable, non-linear relationship with diabetic retinopathy diagnosis. Thus, the experiment shows the effectiveness of HAFT from another angle.

4.2.7 Short- vs. Long-Term Gain Trade-Off. This experiment aims to answer: *How does the trade-off between short-term and long-term gains affect the sequential decision-making process of HAFT?* We select the Airfoil dataset as a candidate for this case study and demonstrate a 5-step feature transformation process. Table 2 shows the exploration process with each step’s immediate and cumulative performance gains. We observe that in step 2, the transformation of U_∞ into $\sigma(U_\infty)$ causes the immediate gain to decrease by -0.2% , while in step 4, this transformation contributes to improving the cumulative gain by a substantial 2.5%. A plausible explanation is that our multi-agent reinforcement learning framework expands the exploration depth during the search process, while the reward-guided schema directs the search to focus on cumulative gains rather than short-sighted decisions. This experiment demonstrates that our collaborative multi-agent system enables the model to balance short-term and long-term gains, allowing sophisticated feature space exploration where initial transformation steps may temporarily reduce performance but yield better overall results.

4.2.8 Study of the Hyperparameter Sensitivity of HAFT. This experiment aims to answer: *To what extent is the performance of HAFT sensitive to the transformer encoder layer number C and the step size M ?* We configured the transformer encoder layer number C from 1 to 9 and the step size M from 10 to 18, then trained HAFT on the SpectF dataset. The performance metrics, including Precision, Recall, and F1, are reported in Figure 8. We observe that HAFT is not sensitive to encoder layer numbers. The plausible explanation is that a single layer of the transformer encoder is sufficiently complex to capture interactions between features and make informed decisions. Additionally, we find that HAFT is robust to training step size. The underlying reason for this observation is that HAFT can

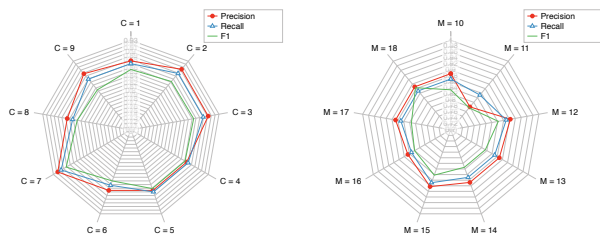
transform informative features without simplifying or complicating the transformation due to variations in the number of steps. And it tends to make decisions based on feature quality rather than the number of operations allowed. Thus, this experiment demonstrates that HAFT is not sensitive to these distinct parameter settings, the learning process of HAFT is relatively robust and stable.

Table 2: Short- vs. Long-Term Gain Trade-Off

Step	f_1	Op	f_2	New	$\Delta(\%)^a$	Cum. (%) ^b
1	c	sin	–	$\sin(c)$	+0.9%	+0.9%
2	U_∞	σ	–	$\sigma(U_\infty)$	–0.2%	+0.7%
3	δ	exp	–	$\exp(\delta)$	+1.8%	+2.5%
4	$\sin(c)$	/	$\sigma(U_\infty)$	$\frac{\sin(c)}{\sigma(U_\infty)}$	+2.5%	+5.0%
5	α	square	–	α^2	+1.3%	+6.3%

^a Immediate change in validation accuracy.

^b Cumulative change from the baseline.



(a) Number of Transformer Layers C (under $M = 15$) (b) Steps per Episode M (under $C = 2$)

Figure 8: The hyperparameter sensitivity test on SpectF

5 Related Works

Automated Feature Transformation aims to refine or augment the original feature space so that machine learning models can more effectively capture complex, high-order relationships among variables. Traditionally, feature transformation techniques fall into two broad categories: latent representation learning-based and feature transformation-based approaches. Latent representation learning-based methods, as demonstrated in [2, 13], focus on learning an optimized, often high-dimensional latent space where feature interactions are implicitly encoded. While these methods are known to boost predictive accuracy, the resulting representations can be challenging to interpret or directly trace back to the original input space. In contrast, feature transformation-based methods [1, 17, 19, 37, 42] generate new features using arithmetic or aggregate operations. Although these methods yield traceable features, they often encounter an exponentially growing search space problem and become inefficient when dealing with large feature sets. In contrast to previous approaches, our attention-based feature crossing strategy not only captures the inherent relationships among features but also scales efficiently. This is achieved by employing cascading agents guided by a shared critic to learn effective feature interaction policies.

Reinforcement Learning investigates how intelligent agents should act within an environment to maximize the expected cumulative reward [31, 39, 41]. Based on the learned policy, reinforcement learning algorithms can be classified into two main categories:

value-based and policy-based. Value-based algorithms [28, 35] estimate the value of states or state-action pairs to facilitate action selection, whereas policy-based algorithms [32] learn a probability distribution that maps states to actions. Furthermore, the actor-critic framework [30] combines the strengths of both approaches. While single-agent reinforcement learning has seen remarkable success, recent work increasingly focuses on multi-agent settings [40] where multiple agents collaborate toward a shared goal. However, variations in observations, actions, or rewards often arise, making effective communication critical for coordination and overall performance. Foerster et al. [9] introduced RIAL and DIAL to facilitate communication among agents. Building on this, Foerster et al. [10] proposed the COMA, employing a centralized critic and a counterfactual baseline for credit assignment. This design supports effective coordination even when agents have distinct reward functions. Lowe et al. [26] extended the actor-critic paradigm by implementing a centralized critic for each agent and allowing them to learn continuous policies, improving the scalability and flexibility of MARL systems. Moreover, Lyu et al. [27] found that centralized critics do not consistently outperform their decentralized counterparts across various evaluation domains. Recent advances in the MARL field, such as the theoretical formulation and empirical adaptation of PPO to cooperative multi-agent settings [23, 48], and Asynchronous Action Coordination [49], have accelerated research progress in this area. Overall, these studies underscore the importance of communication, collaboration, and effective credit assignment in the context of MARL. In our work, we adopt a similar communication mechanism by introducing a customized cascading design alongside a shared critic to address our feature transformation task.

6 Conclusion

In this paper, we propose a heterogeneous multi-agent framework for automated feature transformation, designed to effectively refine the feature space and enhance downstream task performance. The core of this framework is a cascading agent structure consisting of two feature agents and one operation agent, which collaborate to explore feature transformation strategies and optimize the feature space. We customize heterogeneous agent structures for selecting candidate features and operations, enabling the agents to learn more intelligent and reliable policies for feature transformation. To further enhance communication among the agents, we develop a shared critic structure that evaluates each agent’s decisions based on global feature space information and the decisions of other agents. To adapt to the dynamically expanding feature space, we implement a multi-head attention-based agent structure to efficiently select suitable features. Besides that, we propose a state encoding technique to enhance the learning process of RL agents. Extensive experiments demonstrate that HAFT effectively refines the original feature space while exhibiting excellent scalability. The shared critic mechanism plays a crucial role in enhancing agent communication, leading to improved policies. Moreover, state encoding enhances the performance of reinforcement learning, enabling the generation of effective feature crossing strategies. In the future, enhancing generalization and adapting to dynamic data environments will be promising directions for further exploration.

References

- [1] Ehtesamul Azim, Dongjie Wang, Kunpeng Liu, Wei Zhang, and Yanjie Fu. 2024. Feature interaction aware automated data representation transformation. In *Proceedings of the 2024 SIAM International Conference on Data Mining (SDM)*. SIAM, 878–886.
- [2] Yoshua Bengio, Aaron Courville, and Pascal Vincent. 2013. Representation learning: A review and new perspectives. *IEEE transactions on pattern analysis and machine intelligence* 35, 8 (2013), 1798–1828.
- [3] David M Blei, Andrew Y Ng, and Michael I Jordan. 2003. Latent dirichlet allocation. *Journal of machine Learning research* 3, Jan (2003), 993–1022.
- [4] Leo Breiman. 2001. Random forests. *Machine learning* 45, 1 (2001), 5–32.
- [5] Tianqi Chen and Carlos Guestrin. 2016. Xgboost: A scalable tree boosting system. In *Proceedings of the 22nd acm sigkdd international conference on knowledge discovery and data mining*. 785–794.
- [6] Xiangning Chen, Qingwei Lin, Chuan Luo, Xudong Li, Hongyu Zhang, Yong Xu, Yingnong Dang, Kaixin Sui, Xu Zhang, Bo Qiao, et al. 2019. Neural feature search: A neural architecture for automated feature engineering. In *2019 IEEE International Conference on Data Mining (ICDM)*. IEEE, 71–80.
- [7] Corinna Cortes and Vladimir Vapnik. 1995. Support-vector networks. *Machine learning* 20, 3 (1995), 273–297.
- [8] Thomas Cover and Peter Hart. 1967. Nearest neighbor pattern classification. *IEEE transactions on information theory* 13, 1 (1967), 21–27.
- [9] Jakob Foerster, Ioannis Alexandros Assael, Nando De Freitas, and Shimon Whiteson. 2016. Learning to communicate with deep multi-agent reinforcement learning. *Advances in neural information processing systems* 29 (2016).
- [10] Jakob Foerster, Gregory Farquhar, Triantafyllos Afouras, Nantas Nardelli, and Shimon Whiteson. 2018. Counterfactual multi-agent policy gradients. In *Proceedings of the AAAI conference on artificial intelligence*, Vol. 32.
- [11] Yanjie Fu, Dongjie Wang, Hui Xiong, and Kunpeng Liu. 2024. Tabular data-centric ai: Challenges, techniques and future perspectives. In *Proceedings of the 33rd ACM International Conference on Information and Knowledge Management*.
- [12] Yang Gao, Dongjie Wang, Scott Piersall, Ye Zhang, and Liqiang Wang. 2025. GPT-FT: An Efficient Automated Feature Transformation Using GPT for Sequence Reconstruction and Performance Enhancement. *arXiv preprint arXiv:2508.20824* (2025).
- [13] Huifeng Guo, Ruiming Tang, Yunming Ye, Zhenguo Li, and Xiuqiang He. 2017. DeepFM: a factorization-machine based neural network for CTR prediction. *arXiv preprint arXiv:1703.04247* (2017).
- [14] Arthur E Hoerl and Robert W Kennard. 1970. Ridge regression: Biased estimation for nonorthogonal problems. *Technometrics* 12, 1 (1970), 55–67.
- [15] Franziska Horn, Robert Pack, and Michael Rieger. 2020. The autofeat python library for automated feature engineering and selection. In *Machine Learning and Knowledge Discovery in Databases: International Workshops of ECML PKDD 2019, Würzburg, Germany, September 16–20, 2019, Proceedings, Part I*. Springer, 111–120.
- [16] Jeremy Howard. 2022. Kaggle Dataset Download [EB/OL]. <https://www.kaggle.com/datasets>.
- [17] Xuanming Hu, Dongjie Wang, Wangyang Ying, and Yanjie Fu. 2024. Reinforcement Feature Transformation for Polymer Property Performance Prediction. In *Proceedings of the 33rd ACM International Conference on Information and Knowledge Management*. 4538–4545.
- [18] Xiaohan Huang, Dongjie Wang, Zhiyuan Ning, Ziyue Qiao, Qingqing Long, Haowei Zhu, Yi Du, Min Wu, Yuanchun Zhou, and Meng Xiao. 2025. Collaborative Multi-Agent Reinforcement Learning for Automated Feature Transformation with Graph-Driven Path Optimization. *arXiv preprint arXiv:2504.17355* (2025).
- [19] Xiaohan Huang, Dongjie Wang, Zhiyuan Ning, Ziyue Qiao, Qingqing Long, Haowei Zhu, Min Wu, Yuanchun Zhou, and Meng Xiao. 2024. Enhancing Tabular Data Optimization with a Flexible Graph-based Reinforced Exploration Strategy. *arXiv preprint arXiv:2406.07404* (2024).
- [20] James Max Kanter and Kalyan Veeramachaneni. 2015. Deep feature synthesis: Towards automating data science endeavors. In *2015 IEEE international conference on data science and advanced analytics (DSAA)*. IEEE, 1–10.
- [21] Udayan Khurana, Horst Samulowitz, and Deepak Turaga. 2018. Feature engineering for predictive modeling using reinforcement learning. In *Proceedings of the AAAI Conference on Artificial Intelligence*, Vol. 32.
- [22] Udayan Khurana, Deepak Turaga, Horst Samulowitz, and Srinivasan Parthasarathy. 2016. Cognito: Automated feature engineering for supervised learning. In *2016 IEEE 16th international conference on data mining workshops (ICDMW)*. IEEE, 1304–1307.
- [23] Jakob Grudzien Kuba, Ruiqing Chen, Muning Wen, Ying Wen, Fanglei Sun, Jun Wang, and Yaodong Yang. 2021. Trust region policy optimisation in multi-agent reinforcement learning. *arXiv preprint arXiv:2109.11251* (2021).
- [24] Chih-Jen Lin. 2022. LibSVM Dataset Download [EB/OL]. <https://www.csie.ntu.edu.tw/~cjlin/libsvmtools/datasets/>.
- [25] Rui Liu, Rui Xie, Zijun Yao, Yanjie Fu, and Dongjie Wang. 2025. Continuous optimization for feature selection with permutation-invariant embedding and policy-guided search. In *Proceedings of the 31st ACM SIGKDD Conference on Knowledge Discovery and Data Mining V. 2*. 1857–1866.
- [26] Ryan Lowe, Yi I Wu, Aviv Tamar, Jean Harb, OpenAI Pieter Abbeel, and Igor Mordatch. 2017. Multi-agent actor-critic for mixed cooperative-competitive environments. *Advances in neural information processing systems* 30 (2017).
- [27] Xueguang Lyu, Yuchen Xiao, Brett Daley, and Christopher Amato. 2021. Contrastive centralized and decentralized critics in multi-agent reinforcement learning. *arXiv preprint arXiv:2102.04402* (2021).
- [28] Volodymyr Mnih. 2013. Playing atari with deep reinforcement learning. *arXiv preprint arXiv:1312.5602* (2013).
- [29] Public. 2022. OpenML Dataset Download [EB/OL]. <https://www.openml.org>.
- [30] John Schulman, Filip Wolski, Prafulla Dhariwal, Alec Radford, and Oleg Klimov. 2017. Proximal policy optimization algorithms. *arXiv preprint arXiv:1707.06347* (2017).
- [31] Richard S Sutton. 2018. Reinforcement learning: An introduction. *A Bradford Book* (2018).
- [32] Richard S Sutton, David McAllester, Satinder Singh, and Yishay Mansour. 1999. Policy gradient methods for reinforcement learning with function approximation. *Advances in neural information processing systems* 12 (1999).
- [33] Binh Tran, Bing Xue, and Mengjie Zhang. 2016. Genetic programming for feature construction and selection in classification on high-dimensional data. *Memetic Computing* 8 (2016), 3–15.
- [34] UCI Machine Learning Repository. 2022 [EB/OL]. UCI Dataset Download. <https://archive.ics.uci.edu/>.
- [35] Hado Van Hasselt, Arthur Guez, and David Silver. 2016. Deep reinforcement learning with double q-learning. In *Proceedings of the AAAI conference on artificial intelligence*, Vol. 30.
- [36] Ashish Vaswani, Noam Shazeer, Niki Parmar, Jakob Uszkoreit, Llion Jones, Aidan N Gomez, Łukasz Kaiser, and Illia Polosukhin. 2017. Attention is all you need. *Advances in neural information processing systems* 30 (2017).
- [37] Dongjie Wang, Yanjie Fu, Kunpeng Liu, Xiaolin Li, and Yan Solihin. 2022. Group-wise reinforcement feature generation for optimal and explainable representation space reconstruction. In *Proceedings of the 28th ACM SIGKDD Conference on Knowledge Discovery and Data Mining*. 1826–1834.
- [38] Dongjie Wang, Meng Xiao, Min Wu, Yuanchun Zhou, Yanjie Fu, et al. 2023. Reinforcement-enhanced autoregressive feature transformation: Gradient-steered search in continuous space for postfix expressions. *Advances in Neural Information Processing Systems* 36 (2023), 43563–43578.
- [39] Mo Wang, Ye Zhang, Jinlong He, Yupeng Zhou, Niantong Li, Jianan Wang, Yifei Sun, and Minghao Yin. 2026. Optimizing Aesthetic Perception through Human-AI Teaming for Subtle Dimension Identification in Art Annotation. *IEEE Transactions on Learning Technologies* (2026).
- [40] Muning Wen, Jakob Kuba, Runji Lin, Weinan Zhang, Ying Wen, Jun Wang, and Yaodong Yang. 2022. Multi-agent reinforcement learning is a sequence modeling problem. *Advances in Neural Information Processing Systems* 35 (2022), 16509–16521.
- [41] Marco A Wiering and Martijn Van Otterlo. 2012. Reinforcement learning. *Adaptation, learning, and optimization* 12, 3 (2012), 729.
- [42] Meng Xiao, Dongjie Wang, Min Wu, Kunpeng Liu, Hui Xiong, Yuanchun Zhou, and Yanjie Fu. 2024. Traceable group-wise self-optimizing feature transformation learning: A dual optimization perspective. *ACM Transactions on Knowledge Discovery from Data* 18, 4 (2024), 1–22.
- [43] Meng Xiao, Dongjie Wang, Min Wu, Ziyue Qiao, Pengfei Wang, Kunpeng Liu, Yuanchun Zhou, and Yanjie Fu. 2023. Traceable automatic feature transformation via cascading actor-critic agents. In *Proceedings of the 2023 SIAM International Conference on Data Mining (SDM)*. SIAM, 775–783.
- [44] Meng Xiao, Dongjie Wang, Min Wu, Pengfei Wang, Yuanchun Zhou, and Yanjie Fu. 2023. Beyond discrete selection: Continuous embedding space optimization for generative feature selection. In *2023 IEEE International Conference on Data Mining (ICDM)*. IEEE, 688–697.
- [45] Wangyang Ying, Dongjie Wang, Xuanming Hu, Yuanchun Zhou, Charu C Aggarwal, and Yanjie Fu. 2024. Unsupervised generative feature transformation via graph contrastive pre-training and multi-objective fine-tuning. In *Proceedings of the 30th ACM SIGKDD Conference on Knowledge Discovery and Data Mining*. 3966–3976.
- [46] Wangyang Ying, Dongjie Wang, Kunpeng Liu, Leilei Sun, and Yanjie Fu. 2023. Self-optimizing feature generation via categorical hashing representation and hierarchical reinforcement crossing. In *2023 IEEE International Conference on Data Mining (ICDM)*. IEEE, 748–757.
- [47] Wangyang Ying, Cong Wei, Nanxu Gong, Xinyuan Wang, Haoyue Bai, Arun Vignesh Malarkkan, Sixun Dong, Dongjie Wang, Denghui Zhang, and Yanjie Fu. 2025. A survey on data-centric ai: Tabular learning from reinforcement learning and generative ai perspective. *arXiv preprint arXiv:2502.08828* (2025).
- [48] Chao Yu, Akash Velu, Eugene Vinitzky, Jiaxuan Gao, Yu Wang, Alexandre Bayen, and Yi Wu. 2022. The surprising effectiveness of ppo in cooperative multi-agent games. *Advances in neural information processing systems* 35 (2022), 24611–24624.
- [49] Bin Zhang, Hangyu Mao, Lijuan Li, Zhiwei Xu, Dapeng Li, Rui Zhao, and Guoliang Fan. 2024. Sequential asynchronous action coordination in multi-agent systems: A stackelberg decision transformer approach. In *Forty-first International Conference*

on Machine Learning.

- [50] Guanghui Zhu, Zhuoer Xu, Chunfeng Yuan, and Yihua Huang. 2022. DIFER: differentiable automated feature engineering. In *International Conference on Automated Machine Learning*. PMLR, 17–1.